Enhancement and Directionality of Spontaneous Emission in Hybrid Self-Assembled Photonic–Plasmonic Crystals**

Martín López-García, Juan F. Galisteo-López, Alvaro Blanco, Jorge Sánchez-Marcos, Cefe López, and Antonio García-Martín*

At variance with expensive and time-consuming fabrication methods used in the microelectronic industry, material micro/nanostructuration using colloidal particles has become a widespread approach to produce two-dimensional (2D) periodic structures with a large variety of topologies, which could find applications in many different fields, such as biosensing or microelectronics.[1] Regarding the field of photonics, where the aim is to control light propagation and emission, 2D periodic systems fabricated from monolayers (ML) of dielectric spheres have been thoroughly investigated over the last few years. Their use as photonic crystals (PCs)[2] has been explored both theoretically[3] and experimentally[4–7] and their potential use as devices to modify the emission from films of semiconductor nanocrystals[8] or as microlens arrays to enhance light extraction from light-emitting diodes (LEDs)[9] has been recently demonstrated.

Nanostructuration based on self-assembly techniques has also been exploited in the fabrication of plasmonic structures. Due to the sensitivity of these systems to the metal topology, the fine degree of control that self-assembled samples offer, combined with other growth techniques, such as electrochemical deposition, can yield structures with novel functionalities. Systems of ordered metal nanovoids have proven to be an efficient way to control the dispersion relation of surface plasmons combining both localized and delocalized plasmons.[10,11] Also, periodically structured metals obtained in this way have been successfully used as substrates for surface-enhanced Raman spectroscopy (SERS).[12] Recently, the combination of photonic and plasmonic systems has been demonstrated as a means to obtain impressive field enhancements at subwavelength scales employing hybrid plasmonic–photonic modes. In these systems, losses associated with plasmons are avoided and applications as waveguides[13] or nanolasers[14] have been put forward. Similarly, one can fabricate self-assembled MLs of dielectric spheres deposited over plasmon-supporting substrates where photonic, plasmonic, and hybrid modes coexist.[15,16]

In this Communication, we demonstrate how spontaneous emission from organic molecules in 2D plasmonic–photonic crystals can be strongly modified. To that end, we study the emission characteristics of MLs of dye-doped polystyrene (PS) spheres deposited on thin gold substrates. In these systems, modes are divided into waveguide-like (WG) modes, associated with the dielectric PCs, plasmonic-like (SPP) modes, localized at the metal interface, and hybrid modes (WG–SPP). At variance with References [13] and [14], we consider hybrid WG–SPP modes to be those in which electric field extends both into the spheres and the metal surface.[15,16] The dispersion relation of the system is obtained from angle- and polarization-resolved reflectivity measurements and the nature of each mode is retrieved by comparing experimental results with finite-difference time-domain (FDTD) calculations. We have also measured photoluminescence (PL) spectra from the samples and obtained a strong enhancement as compared to reference PCs deposited on plain, flat dielectric substrates. Such enhancement is present for those modes whose electric field extends into the optically active spheres. Hence, the PL follows the dispersion of such modes, becoming highly directional and with a well defined polarization.

2D PCs based on dielectric spheres have been widely studied over the past few years.[3–7,17] In particular, free-standing structures ($n_{sub} = 1$) are known to sustain both guided and leaky propagating modes, where the former are vertically confined by total internal reflection, whereas the latter leak energy through coupling to the modes of the surrounding medium. Given that no coupling is possible from guided modes to the isotropic surrounding media (and vice versa), far-field

[*] M. López-García, Dr. J. F. Galisteo-López, Dr. A. Blanco, Dr. J. Sánchez-Marcos, Prof. C. López
Instituto de Ciencia de Materiales de Madrid (CSIC) and Unidad Asociada CSIC-U. Vigo
C/Sor Juana Inés de la Cruz 3, 28049 Madrid (Spain)
E-mail: cefe@icmm.csic.es
Dr. A. García-Martín
Instituto de Microelectrónica de Madrid (IMM-CSIC)
C/ Isaac Newton 8, 28760 Tres Cantos, Madrid (Spain)

[**] J. F. Galisteo-López was supported by the JAE Postdoctoral Program. M. López-García was supported by the FPI PhD program from the MICINN. This work was supported by the Spanish MICINN CSD2007-0046 (Nanolight.es) and MAT2006-09062 projects. A. García-Martín also acknowledges financial support from the Spanish MICINN ("MAGPLAS" MAT2008-06765-C02-01/NAN, Funcoat Consolider Ingenio 2010 CSD2008-00023), and European Commission (NMP3-SL-2008-214107-Nanomagma).

DOI: 10.1002/smll.201000216

measurements only yield information on leaky modes. For the free-standing scenario, leaky modes appear as peaks (dips) in a far-field reflectance (transmittance) spectrum.[3,19] For the case of a ML deposited on a semi-infinite dielectric substrate, which is a more realistic scenario from the point of view of fabrication than that of a free-standing one, losses into the substrate are known to be much larger. Eventually, in the event that $n_{sub} > n_{eff}$ (where n_{eff} is the average refractive index of the ML), no guided modes are to be found. This means that light confinement in the ML will not occur and its use will be restricted.

In the present work, we consider samples where the sphere ML is grown on a metallic substrate (see Figure 1). As for the case of the finite dielectric substrate,[3] the modes of this system can be viewed as a result of the coupling between substrate and ML modes. While, in the past, this system has been mainly studied as a starting point for fabricating plasmonic systems with complex topologies,[15] herein, we will explore its optical response per se and without further processing or modification. Figure 2a shows experimental and calculated reflection spectra for a ML of 520-nm spheres grown on gold. Here, the modes of the system to which we couple at normal incidence appear as dips in a nearly flat background of high reflectance. The background reproduces the optical response of the gold film, where the drop in reflectance for higher frequencies corresponds to the onset of absorption. For $\omega > 1$ (where the reduced frequency $\omega = \sqrt{3}d_{sph}/(2\lambda)$), out-of-plane diffraction takes place and there is an additional drop in reflected intensity, together with a reduced field confinement inside the spheres. The dips present in the spectra correspond to light coupling to the modes of the system and therefore not being reflected. The spectral position of experimental and calculated dips show good overall agreement with deviations of ≈1.5%, below the 3% polydispersity of the spheres. Experimental peaks are broader than calculated ones, possibly due to the presence of small lattice distortions generated during the growth process.

In order to explore the nature of each mode, we calculated the spatial distribution of their total field intensity. Figure 2b shows the field profile in the direction normal to the 2D periodicity. Here we see how modes G1 ($\omega = 0.67$) and G2 ($\omega = 0.72$) correspond to SPP- and WG-like modes, respectively, with the electric field concentrated at the metal–ML interface and at the sphere centre. On the other hand, G3 ($\omega = 0.77$) clearly corresponds to a hybrid mode, with a more complex field distribution extending both into the metal–ML interface and the spheres. Hence, if an emitter is placed inside the sample, one would expect an enhancement in emission for those frequencies corresponding to the leaky modes. The spectral distribution of the enhancement will certainly depend on the spatial overlap between the modes and the emitter which, in our particular case, is homogeneously distributed throughout the sphere volume.

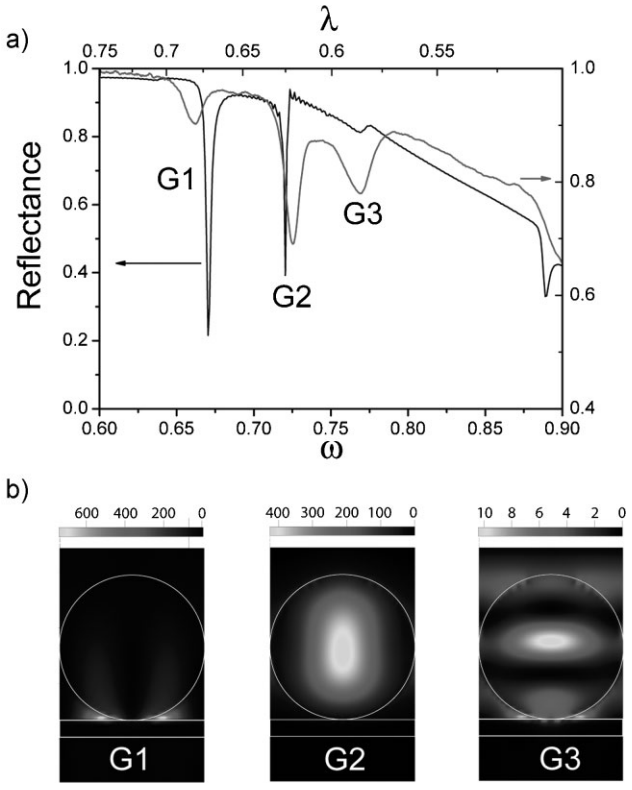

Figure 2. a) Calculated (black curve) and measured (grey curve) normal-incidence reflection spectra of a ML of 520-nm PS spheres grown on a gold substrate. b) Total-field-intensity distribution of selected modes (as indicated in Figure 2a).

If we pay attention to the absolute values of the calculated fields, we can see how the field enhancement obtained for the WG- and SPP-like modes are one order of magnitude larger than that for the hybrid mode. We have also performed similar calculations for the ideal case of the free-standing ML and found values four times smaller than in the samples under study. One can safely assume that the present system should perform much better than the ideal case of the free-standing ML considered up to now in terms of light confinement.

Now that the optical response of the passive system has been studied, we discuss its emission properties when an isotropic

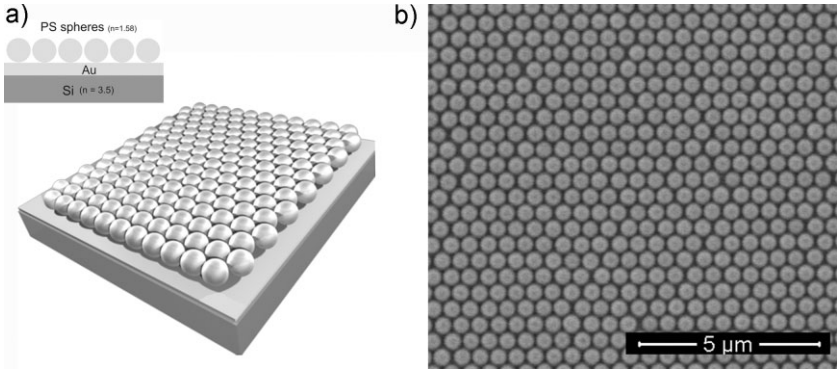

Figure 1. a) System under study consisting of a close-packed arrangement of dielectric spheres deposited on a silicon substrate on which a thin (60 nm) gold film had been deposited. b) Scanning electron microscopy (SEM) image of an actual sample made from 520-nm PS spheres.

emitter is placed inside the spheres so that the emission overlaps spectrally with the modes discussed above. Prior to analyzing the emission spectra, we have to consider that, due to the way the emitter is distributed in our samples (i.e., within the volume of the dielectric spheres), only a small portion of the total amount of molecules will be near the metal surface, namely those located at the contact point between the spheres and gold.

Figure 3 shows unpolarized emission spectra at normal incidence for a ML grown on a gold substrate and on a silicon substrate, together with a reflectance spectrum for the gold-substrate sample. For the silicon sample, no enhancement is observed in the spectral range of interest. This is in accordance with the low field enhancement expected within the spheres in this type of sample due to leakage into the substrate. On the contrary, for the sample grown on the gold substrate, a large enhancement of the emission takes place for the mode located at $\omega = 0.72$, which, as explained before, corresponds to a WG-like mode. For this mode, the electric field is mainly confined in the sphere, where the emitter is homogeneously distributed. A 20× enhancement in emission is observed for this mode when compared with that of the reference sample grown on silicon. Emission is also enhanced over the background for the mode at $\omega = 0.77$, though much less than for the previous case. This is in agreement with the fact that this corresponds to a hybrid mode with a much smaller electric field confinement (see Figure 2). Although one would expect a larger enhancement associated with the WG-like mode (notice that the total electric field at the sphere center is 40 times that of the hybrid one), it should be noted that the WG-like mode lies at the emission tail while the hybrid one lies at its spectral maximum. A barely noticeable enhancement in emission is observed for those frequencies corresponding to the SPP-like mode. The reason for this is twofold: on one hand, the spatial overlap between the electric field and the dye molecules is at a minimum and, on the other hand, frequencies corresponding to this mode lie far into the low-energy tail of the dye's emission. In fact, if emitters were distributed near the gold film, a stronger enhancement would be expected for SPP and hybrid SPP–WG modes.

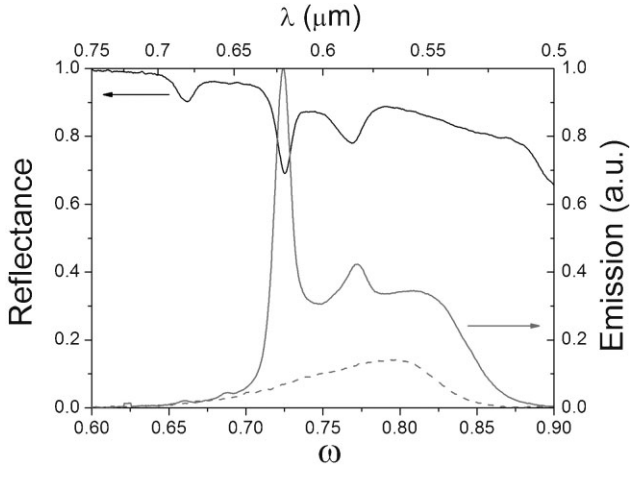

Figure 3. Normal-incidence reflection (black curve) and emission (grey solid curve) from a ML of 520-nm PS spheres deposited on a gold substrate. The emission from a ML of identical spheres grown on a silicon substrate (grey dashed curve) is plotted for comparison.

The observed enhancement in emission could certainly be improved in the future, both by choosing plasmon-supporting surfaces (such as silver), which would minimize absorption in the visible range, and optimizing the crystalline quality of the periodic dielectric lattice, which would reduce the effect of unwanted disorder.

Next, we experimentally studied the dispersion relation of the samples grown on gold substrates, which provide information on the set of pairs (ω,k) available for each mode. Results are shown in Figure 4 as contour plots. We have selected the ΓK high-symmetry direction of the hexagonal lattice as being representative of the sample and considered both s (electric field perpendicular to the reflection plane) and p (electric field contained in the reflection plane) polarizations. Similar results were obtained for the other high-symmetry direction of the hexagonal lattice (i.e., ΓM, not shown). Results for both reflection and emission are shown in Figure 4a and b, respectively. If we consider reflectance measurements, we can see how the dispersion of the SPP-like mode appearing at $\omega = 0.67$ for normal incidence is barely noticeable. The WG-like and hybrid modes ($\omega = 0.72$ and $\omega = 0.77$ for normal

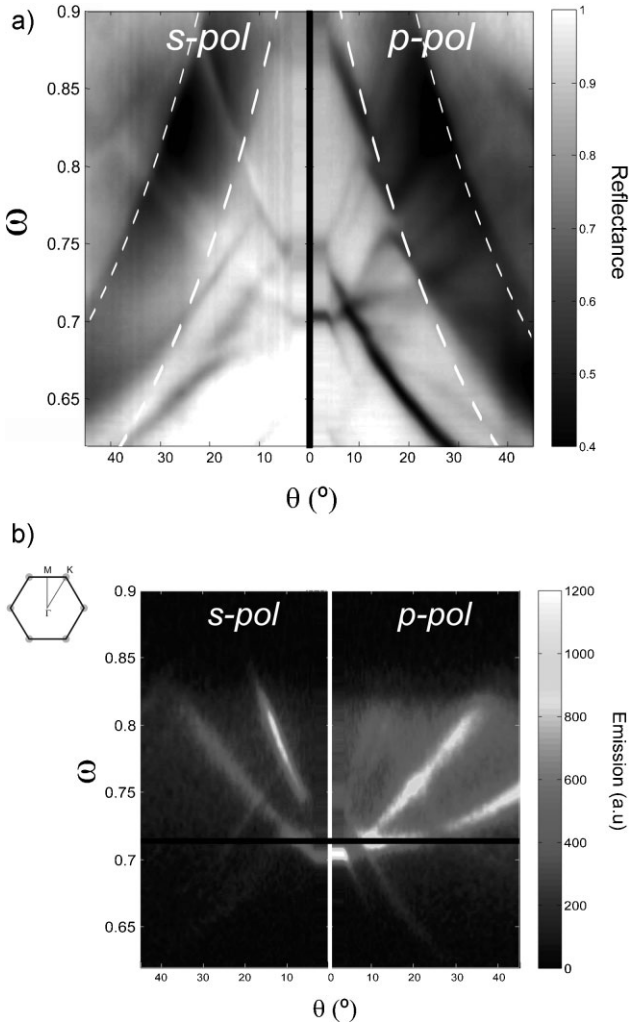

Figure 4. a) Angle-resolved reflectance measurements along the ΓK direction for both s (left) and p polarizations (right panel). b) Angle-resolved emission in identical conditions to the reflectance ones.

incidence, respectively) are degenerate at $k = 0$ and branch into several modes with different polarization as we depart from normal incidence ($k = 0$).

The effect of out-of-plane diffraction is now also evident as an abrupt decrease in reflectance, which appears as a dark band in the contour plot. Two sets of dashed lines delimit this band, where the low-energy one corresponds to the onset of diffraction of the specular beam extracted from the diffraction condition by the different periodicities present in the ML. Such diffracted light is not collected in the specular direction. Above a certain collection angle, light diffracted by smaller angles re-enters the fiber and the collected intensity rises again. This is indicated by the high-energy dashed line. Finally, it is also worth mentioning the appearance of anticrossings between modes having the same symmetry character, indicating the high crystalline quality of the samples.

If we now consider angle-resolved emission measurements (see Figure 4b), we can see how emission is channeled only by certain modes, as happened for normal incidence. This fact provides both directionality and polarization selectivity of the dye's emission. For p-polarized light, it can be observed how most of the dye's emission couples to two modes originating from the WG-like mode, G2, in Figure 2. For s-polarized light, emission couples mainly to two modes originating from the G2 and G3 modes respectively, although with different efficiency. As we mentioned above, these two modes have a WG (G2) and a hybrid (G3) nature. No emission couples to the plasmon-like modes observed at normal incidence since, as we increase the angle, the energy of these modes decreases (see Figure 4a) and hence we move away from the dye's emission spectral range.

Some discrepancies in the correspondence between dips in emission and peaks of enhanced emission can be observed in Figure 4, particularly for p polarization and angles above 10°. We believe the origin of such discrepancy is twofold. On one hand, some modes may not be excited efficiently in a reflection measurement for symmetry reasons but can efficiently emit once the molecules inside the spheres are excited. On the other hand, out-of-plane diffraction may hamper the observation of certain peaks in reflection as they overlap, an effect which should be more pronounced for the case of p polarization where the out-of-plane diffraction efficiency should be larger, similarly to conventional gratings.

However, the combination of periodic dielectric structures and metallic substrates is not only advantageous from the point of view of enhanced spontaneous emission or polarization selectivity, as we have just seen. Directionality is also a consequence of the channeling of emission through the modes of the sample. This becomes more evident if one plots emission in polar coordinates for a given frequency, as shown in Figure 5. For the case of the reference sample grown on a silicon wafer, we observe a constant angular profile. This is in agreement with calculations for an emitter in a slab of dielectric material. In this situation, one expects a Lambertian distribution, which, for the angular range collected in these experiments, appears as a flat background. Introducing the gold substrate produces an enhanced emission background for those frequencies where no modes are available and a directional enhancement where emission may couple to a mode. For the chosen reduced frequency ($\omega = 0.8$), emission takes place in a reduced angular range close to the normal but, since a wide range of tunability is possible through the periodicity of the dielectric lattice, directionality can be tailored for a given frequency by adjusting the sphere diameter relative to the wavelength.

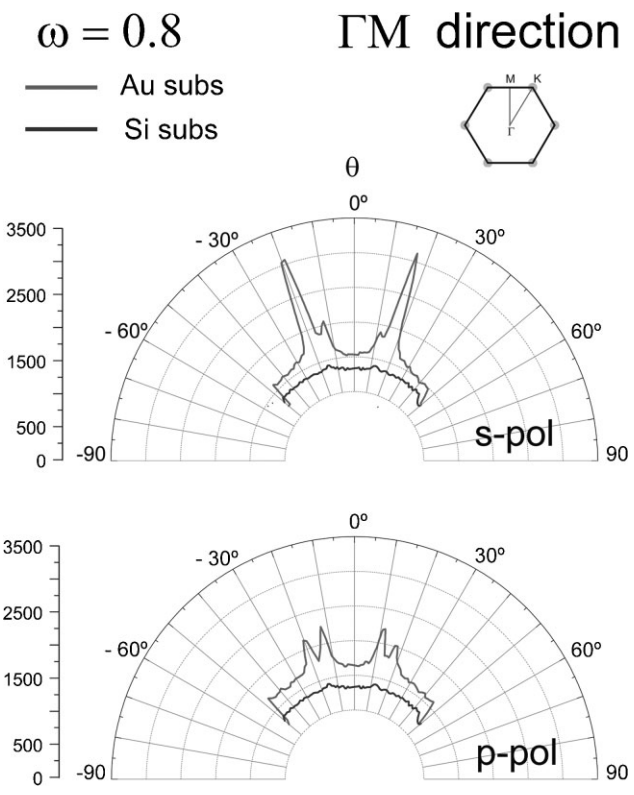

Figure 5. Polar plot for emission from a 520-nm-sphere ML grown on a gold substrate (grey curve) and on a silicon substrate (black curve) for a reduced frequency $\omega = 0.8$ along the ΓM direction in reciprocal space. Inset shows the reciprocal lattice of the system.

In conclusion, we have shown both experimentally and theoretically that MLs of dielectric spheres deposited on metallic substrates can strongly modify the emission of organic dyes contained in the spheres through coupling to hybrid plasmonic–photonic modes of the structure. Emission enhancement due to strong field confinement inside the spheres has been demonstrated together with its polarization dependence. Finally, evidence for the directionality of the emission has been presented. We believe that the economy and ease of fabrication of high-quality samples, together with the possibility of tuning their emission characteristics via the dielectric periodicity, endows this system with the potential to be exploited in future efficient light-emitting devices. Further, appropriately placing the emitter closer to the metal surface (while avoiding quenching effects) would allow the SPP-like modes, which present a better electric-field confinement, to be exploited. Also, in more carefully designed samples, both pump and emission could be tuned to different modes of the sample in order to optimize emission enhancement.

Experimental Section

Sample fabrication: Samples were fabricated by the vertical deposition method,[18] where a rigid substrate is placed vertically

on an aqueous solution of spheres with a sufficiently low concentration (0.08 wt%), so as to produce an ordered ML of spheres as the solvent is evaporated (see Figure 1). The growth process was performed in a furnace with controlled temperature (50 °C) and humidity (20%). We used PS spheres (Duke Scientific) having a diameter of 520 nm and containing an organic dye (Rhodamine 6G) homogeneously distributed throughout their volume. The sphere diameter was chosen in order to place the dye emission in a spectral region of the dispersion relation where the three types of modes present in these structures appear. As substrates, we used 450-μm-thick silicon wafers (ACM) on which a thin gold film (60 nm) was sputtered. In order to secure the adherence of the gold film to the silicon wafer, a 2-nm chrome layer was previously deposited. Atomic force microscopy (AFM) was used to characterize the roughness of the gold layer, which could influence sample quality, and values below 1 nm were obtained. As a reference sample, we employed a ML from the same spheres grown on a silicon substrate without the gold film.

Optical characterization: To optically characterize the samples, angle- and polarization-resolved reflectance measurements were carried out with a large-numerical-aperture (0.75) 40× objective coupled to a microscope. A 1-cm-large image of the back focal plane of the objective was formed outside the microscope and an optical fiber (100-μm-diameter core) was scanned across the image so that different fiber positions provide spectra that can be associated with different angles of incidence/collection.[19] The system was calibrated using a commercial reflection grating with a known lattice parameter. Under these conditions the angular resolution of each measurement was always kept better than 1°. Angle-resolved measurements were collected along different high-symmetry directions for which the sample was oriented employing the hexagonal diffraction pattern characteristic of these systems under monochromatic- or white-light illumination. Angle and polarization emission measurements were collected using the same experimental setup as reflectance ones only; instead of using a tungsten lamp for white-light illumination, a continuous-wave (CW) diode laser with $\lambda = 485$ nm (Picoquant, LDH-P C-485) was used to pump the samples. Such a pump wavelength, although slightly shifted from the absorption maxima of the organic dye (542 nm) provided a good emission signal. The pump power was ≈1.5 mW for all measurements.

Simulations: Numerical simulations were performed with a commercial software (Lumerical FDTD Solutions) from which normal-incidence reflectance spectra were calculated along with the spatial distribution of the total field intensity at those wavelengths at which mode excitation takes place. The presence of the gold layer, together with the possible coupling to localized excitations, makes it necessary to employ a fine grid (≥40 points per wavelength in each direction) as well as a sufficiently long simulation time (≥1 ps). For the calculations, the optical constants employed to simulate gold were taken from ellipsometric measurements performed on substrates grown by the same technique as those used in the present experiments.

Keywords:
directionality · emission · photonics · plasmonics · polarization

[1] Y. Li, W. Cai, G. Duan, *Chem. Mater.* **2008**, *20*, 615.
[2] K. Sakoda, *Optical properties of Photonic Crystals* Springer-Verlag, Berlin **2001**.
[3] Y. Kurokawa, H. Miyazaki, Y. Jimba, *Phys. Rev. B* **2002**, *65*, 201102.
[4] H. T. Miyazaki, H. Miyazaki, K. Ohtaka, T. Sato, *J. Appl. Phys.* **2000**, *87*, 7152.
[5] T. Kondo, M. Hangyo, S. Yamaguchi, S. Yano, Y. Segawa, K. Ohtaka, *Phys. Rev. B* **2002**, *66*, 033111.
[6] X. Wang, C. Neff, E. Graugnard, Y. Ding, J. S. King, L. A. Pranger, R. Tannenbaum, Z. L. Wang, C. J. Summers, *Adv. Mater.* **2005**, *17*, 2103.
[7] Y.-C. Chang, H.-W. Wu, H.-L. Chen, W.-Y. Wang, L.-J. Chen, *J. Phys. Chem. C* **2009**, *113*, 14778.
[8] S. G. Romanov, M. Bardosova, I. M. Povey, C. M. Sotomayor Torres, M. E. Pemble, N. Gaponik, A. Eychmüller, *J. Appl. Phys.* **2008**, *104*, 103118.
[9] P. Kumnorkaew, Y.-K. Ee, N. Tansu, J. F. Gilchrist, *Langmuir* **2008**, *24*, 12150.
[10] T. A. Kelf, Y. Sugawara, J. J. Baumberg, M. E. Abdelsalam, P. N. Barlett, *Phys. Rev. Lett.* **2005**, *95*, 116802.
[11] T. A. Kelf, Y. Sugawara, R. M. Cole, J. J. Baumberg, M. E. Abdelsalam, S. Cintra, S. Mahajan, A. E. Russell, P. N. Barlett, *Phys. Rev. B* **2006**, *74*, 245415.
[12] J. J. Baumberg, T. A. Kelf, Y. Sugawara, S. Cintra, M. E. Abdelsalam, P. N. Barlett, A. E. Russell, *Nano Lett.* **2005**, *5*, 2262.
[13] R. F. Oulton, V. J. Sorger, D. A. Genov, D. F. P. Pile, X. Zhang, *Nat. Photonics* **2008**, *2*, 496.
[14] R. F. Oulton, V. J. Sorger, T. Zentgraf, R.-M. Ma, C. Gladden, L. Dai, G. Bartal, X. Zhang, *Nature* **2009**, *461*, 629.
[15] R. M. Cole, Y. Sugawara, J. J. Baumberg, S. Mahajan, M. E. Abdelsalam, P. N. Barlett, *Phys. Rev. Lett.* **2006**, *97*, 137401.
[16] L. Shi, X. Liu, H. Yin, L. Zi, *Phys. Lett. A* **2010**, *374*, 1059.
[17] M. Inoue, K. Ohtaka, S. Yanagawa, *Phys. Rev. B* **1982**, *25*, 689.
[18] P. Jiang, J. F. Bertone, K. S. Hwang, V. L. Colvin, *Chem. Mater.* **1999**, *11*, 2132.
[19] The present experimental setup is similar to that reported in M. Richard, J. Kasprzak, et al *Phys. Rev. Lett* **2005**, *94*, 187401; in our case however, measurements were done in a reflection-and-emission configuration.

Received: February 9, 2010
Revised: April 26, 2010
Published online: July 27, 2010

